

MUMT 618  
Computational Modeling of Musical Acoustic Systems  
Final report  
Brass Physics and Modeling Techniques

Alberto Acquilino

December 4, 2020

# 1 Introduction

This project proposes to analyze literature studies on the physics of brass musical instruments and on the models that simulate their behavior. In particular, mono- and two-dimensional, linear and non-linear models of the musician's lip vibration production system are studied.

The report is divided into four main parts, each corresponding to a different article in the literature:

- Chapter 2 considers *The Physics of Brasses* by Benade [3]. It introduces the definition of the horn equation, describes methods of measuring input impedance, and discusses experimental results found on brass and cylindrical tubes.
- Chapter 3 analyzes the work by Adachi and Sato [1] on the formulation of two one-dimensional models to simulate the buzzing lips behavior of the brass performer, analyzing the details.
- Chapter 4 describes a second study by Adachi and Sato [2] which defines a two-dimensional model that combines the two models studied in the previous article.
- Chapter 5 considers an article by Rodet and Vergez [7] which describes the non-linearity arising from the airflow inside the mouthpiece via the Hopf theorem.

The following chapters describe for each of these studies the main characteristics and theories in order to provide an overview of the behavior of the instrument in interaction with the musician.

## 2 *The Physics of Brasses* by Arthur H. Benade

Benade's article represents the starting point of this study. It provides a historical background on how brass instruments were conceived and widely used long before the physical laws describing the acoustic behavior of the instrument were expressed. It focuses in particular on cylindrical brass instruments, such as trumpet and trombone, introducing a simplification of the treatment in the case of conical brass instruments, which have a less accentuated flaring profile of the bell. Subsequently, the text describes the evolution of theories formulated in the twentieth century to describe the interaction between the physical, geometric and acoustic variables with the audio spectrum produced by brasses. Finally, it presents the studies of the author himself, experimentally verified, still today a reference point for the state of the art.

### 2.1 Historical background on the horn equation

Brass musical instruments have an ancient history and they are played for a long time. However, no one has ever been able to give an explanation on the physics behind the production of sound until after the eighteenth century. Before, the brass instrument manufacturers were able to identify effective horn shapes and profiles and repair the errors of defective instruments without resorting to sophisticated acoustic knowledge.

The wave equation in cylindrical horns was first discussed by Daniel Bernoulli, Leonhard Euler and Joseph Louis Lagrange in the second half of the eighteenth century. Despite the rapid spread of the ideas of the three physicists, which led to a great development of modern physics, their deductions on the wave equation were not particularly successful in the acoustics science of that period. The study of horn equation for acoustic purposes developed in the early decades of the twentieth century: the American physicist Arthur Gordon Webster published a report on the horn equation in 1919. The interest of that period was mainly on the development of sonar gear in the naval field for military applications and, in the audio field, on the optimization of the loudspeaker profile for applications in the phonograph and radio industries.

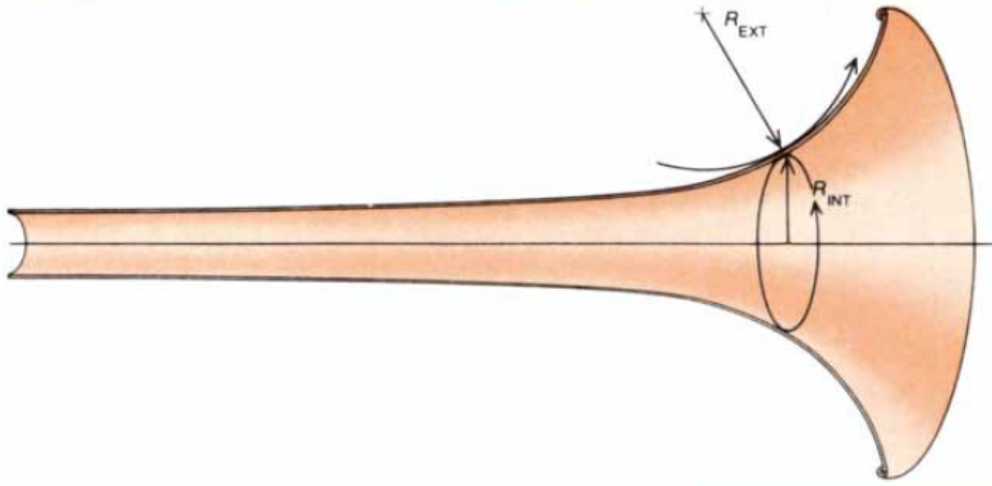


Figure 1: Horn profile shape

However, from the acoustic point of view, a loudspeaker and a brass instrument have to meet different requirements: a loudspeaker horn must be designed to radiate sound efficiently out into the air over a broad range of frequencies from a small source, while in a musical horn the flare of the bell must be designed to trap energy inside the horn, giving strongly marked standing waves at precisely defined frequencies.

The simplified version of the horn equation is defined by:

$$\lambda = \frac{c}{\sqrt{f^2 - U (c/2\pi)^2}} \quad (1)$$

It indicates how the acoustic wavelength  $\lambda$  is related at each point of the horn to the speed of sound  $c$  and to the frequency of the sound produced  $f$ . The horn function  $U$  is a geometric parameter that evolves along the profile of the instrument and is defined as:

$$U = \frac{1}{R_{INT} \cdot R_{EXT}} \quad (2)$$

where  $R_{INT}$  and  $R_{EXT}$  represent the internal and external radius respectively, as indicated in Figure 1.

Equation 1 determines how much of the acoustic energy leaves the horn and how much is reflected back into the horn to produce standing waves inside the instrument. For frequencies below a specific critical value determined by the magnitude of the horn function, the wavelength  $\lambda$  becomes mathematically imaginary, thus the corresponding sound wave becomes strongly attenuated. Therefore, regions with high values of  $U$  may form a barrier to the transmission of waves to the outside. Such waves are reflected into the instrument back to the mouthpiece and produce standing wave inside the instrument.

Figure 2 on the top illustrates the typical profile of a loudspeaker with the orange line, characterized by a catenoidal shape, while in black a trombone profile. At the bottom, the corresponding values of the horn function are reported along the lengths of the profiles. While the loudspeaker presents a rather flat horn function, the acoustical properties of the trombone vary from point to point, even if the two bells are matched to have the same radii at both ends. Indeed, the flaring shape of the trombone bell is designed to save energy inside the horn, thus generating strongly marked standing waves at specific frequencies. This because the higher the value of the function  $U$ , the higher the barrier to sounds of low frequency. Consequently, as shown in the Figure 2, sounds at higher frequency are able to progress farther before they are reflected back by the barrier. In both cases, above a certain frequency, most of the sound energy radiates over the top of the

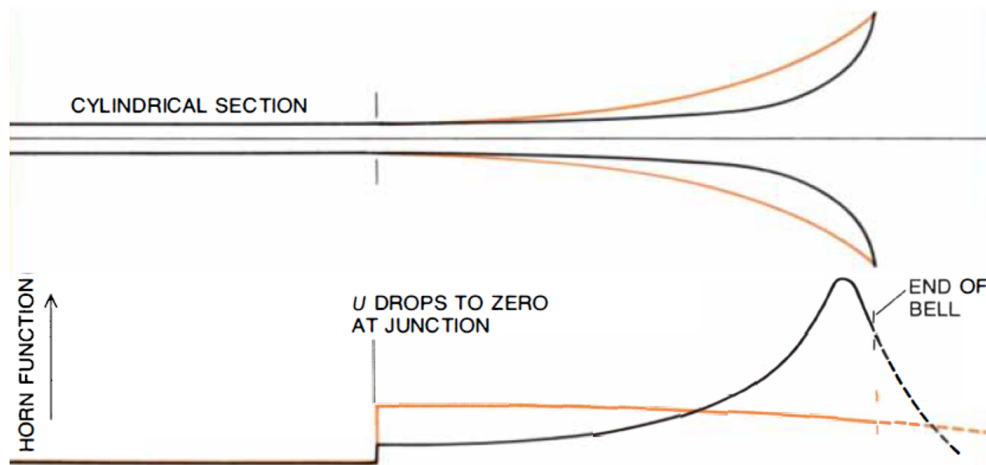


Figure 2: At the top: loudspeaker (orange line) and trombone (black line) profiles along their length. At the bottom: the corresponding horn function curves

barrier, so that the bell of the trombone loses its musically useful character and behaves like a loudspeaker horn.

The wave that is reflected back down the bore of the horn combines with newly injected waves to produce a standing wave. Depending on the interaction between the injected wave and the reflected wave, the pressure disturbance inside the mouthpiece can be large or small. Such disturbances in the mouthpiece characterize the input impedance, which is defined as the ratio between the pressure amplitude set up in the mouthpiece and the corresponding excitatory flow. The impedance of a trumpet-like instrument as a function of the frequency is illustrated at the top of Figure 3. At the bottom, the shape of the air column is shown at the extreme left, while the curves at the right represent the standing-wave patterns that exist in the air column of the instrument at frequencies that produce the maxima and minima in the impedance curve. The impedance depends on whether the sound wave reflected from the bell returns in step or out of step with the oscillatory pressure wave produced in the mouthpiece. At the peaks, the reflected wave is precisely in step with the entering wave, while in correspondence of the minimum impedance values the returning wave and the incoming wave are exactly out of step with each other in the mouthpiece. It can be noted that the number of nodes in the standing-wave pattern increases by one at each impedance peak. Figure 3 also shows that for higher frequencies, the sound wave penetrates more deeply into the bell, before being reflected.

## 2.2 Input impedance: experimental results

The article subsequently describes two systems for measuring the input impedance, one used from 1945 to 1965 by Earle L. Kent while working at C.G. Conn Ltd., and the second described in 1968 by Josef Merhaut, that can be applied also in measurements on woodwind instruments. The input impedance of a cylindrical tube is analyzed (Figure 4 on the left), which shows many evenly spaced input impedance peaks. Such peaks correspond to the natural frequencies of a cylindrical pipe stopped at one end. Resonance peaks become smaller at higher frequencies because frictional and thermal losses inside the tube walls increase with frequency. The energy radiated from the open end of such a pipe is less of 1% of the wall losses. The remainder is trapped inside the tube producing standing waves.

If a trumpet bell is added to the same cylindrical pipe, the impedance response curve becomes like that on the right of Figure 4. The first peak is not shifted, but the frequencies of the other resonances are lowered in a smooth progression because the injected waves penetrate ever more deeply into the bell before being

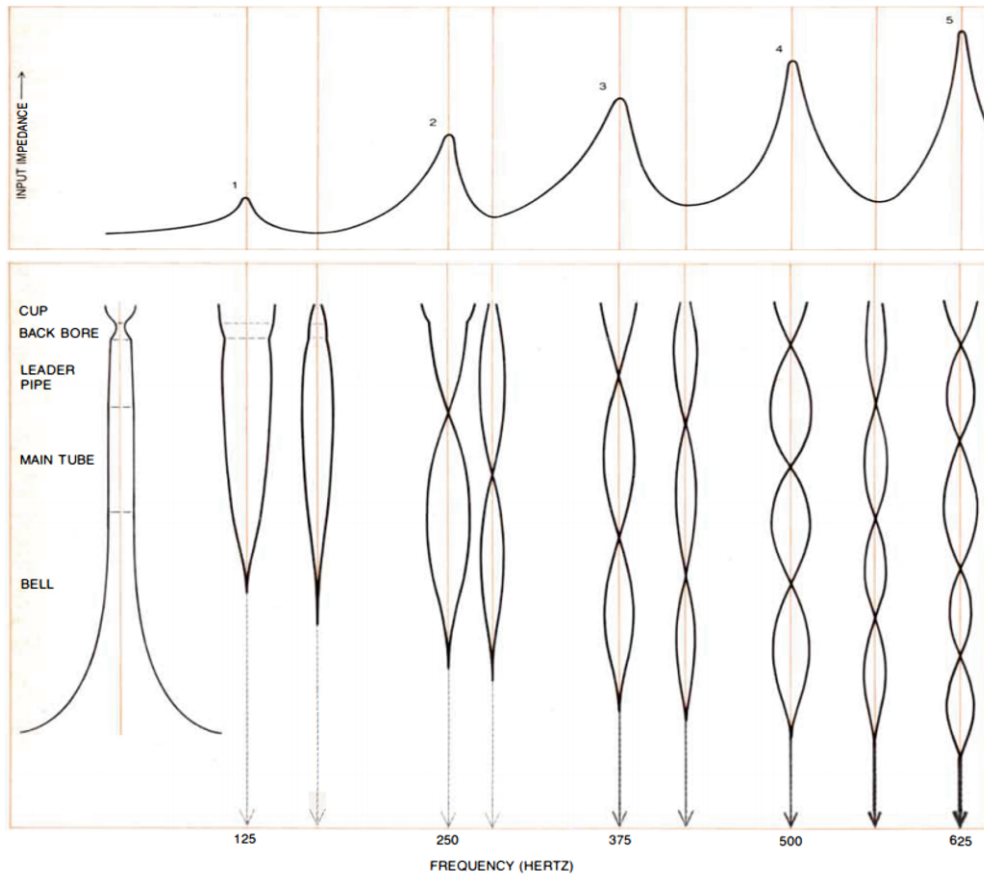


Figure 3: At the top: input impedance curve as a function of the frequency. At the bottom: the corresponding standing wave patterns

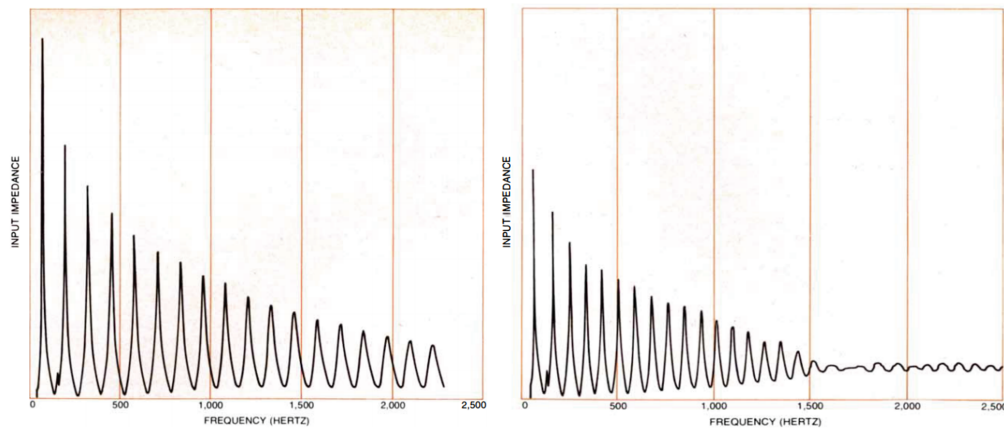


Figure 4: Input impedance curve of a cylindrical pipe (on the left) and of a pipe plus bell system (on the right)

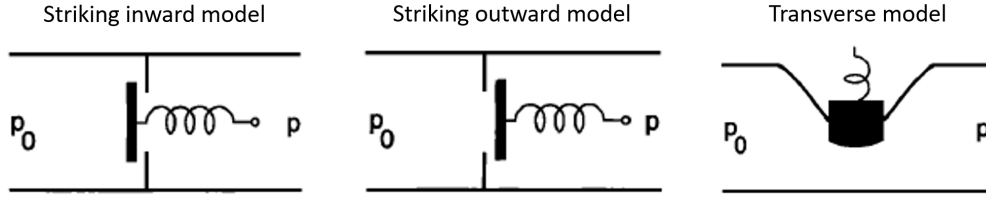


Figure 5: Three different configurations of a pressure-controlled valve in an acoustic tube. In each configuration,  $p_0$  indicates the pressure in the upstream region of the valve, while  $p$  represents the pressure in the downstream region

reflected. In addition, the peaks at higher frequencies are markedly reduced in height because a growing fraction of the energy supply leaks through the bell barrier as the frequency is increased. Therefore in this case, the return wave is weakened not only by wall losses but also by radiation losses, particularly at high frequencies. Above about 1500 hertz, essentially no energy returns from the flaring part of the bell. This means that this part of energy is radiated into the environment.

Finally, the studies by Benade and Worman on the energy distribution between harmonics as the sound intensity varies are presented in the article. They demonstrated that when the player blows very softly, essentially no harmonics are present in the vibration as measured in the mouthpiece. Whereas if the musician plays louder, the amplitude of the second harmonic grows in such a way that for every doubling of the strength of the fundamental component, the second harmonic increases by a factor of four. Similarly, the third harmonic increases in strength by a factor of eight for each doubling in strength of the fundamental, and so on. This theorem fails to give simple results only at very loud playing levels. When the performer plays rather loud, the strengths of the various harmonics have heights that correspond roughly to the heights of the corresponding impedance maxima. They observed that this law is totally independent of all details of the flow control properties of the lips, provided only that the flow is controlled solely by the pressure variations in the mouthpiece.

### 3 *Time-domain simulation of sound production in the brass instrument by Seiji Adachi and Masa-Aki Sato*

This paper investigates the sound production of brass instruments to make up for the lack of understanding of that period and carries out time-domain simulations to show the possibility of physical modeling that synthesizes realistic brass sounds. It analyzes the three different types of valve configurations described by Fletcher [4], shown in Figure 5.

In the striking inward model, used to describe the reed vibration of woodwind instruments, the valve closes in increments of the blowing pressure, while in the striking outward model - also called swinging-door model - the valve opens further. In the transverse model instead the closure of the valve is determined by the Bernoulli pressure. The last two models can be adopted to describe lips vibration for brass instruments. The paper describes these two models independently within linearity conditions, one with the striking outward model and the other adopting the transverse model.

The article presents a set of mathematical equations to represent both models, which is described as a function of the following variables:

- the mouthpiece sound pressure  $p$
- the air volume velocity  $U$  flowing through the lip orifice into the mouthpiece

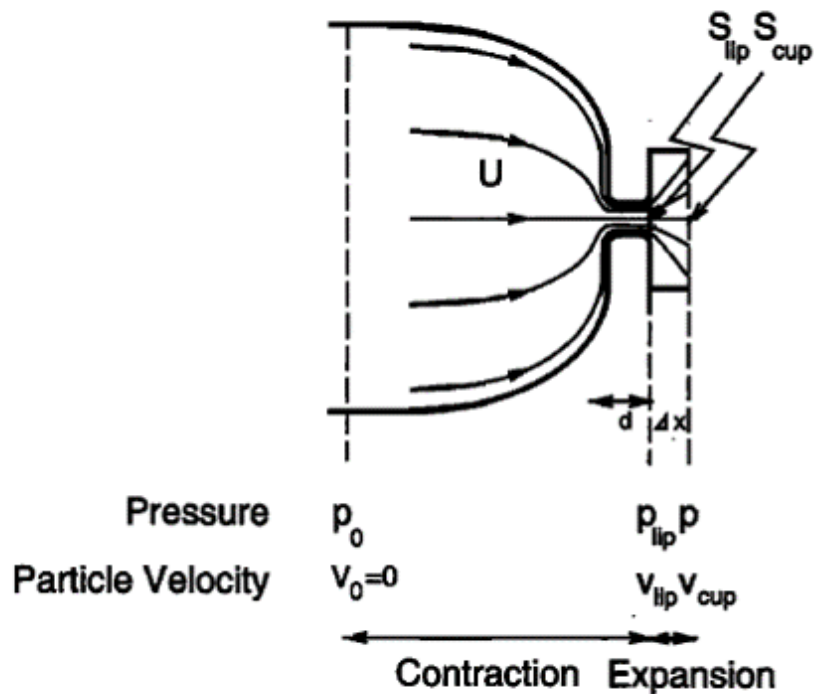


Figure 6: Schematic diagram of mouth, lips and mouthpiece entryway

- the area of the lip orifice  $S_{lip}$

Such a set of equations includes an equation governing air flow through the lip orifice, an equation of lip motion, and an integral equation representing the feedback from the instrument.

### 3.1 Airflow equation

Figure 6 illustrates a scheme of the mouth plus mouthpiece system. The flow  $U$  is generated by the difference between the blowing pressure  $p_0$  and the mouthpiece pressure  $p$ , and also regulated by the area of the lip orifice  $S_{lip}$ . It gets abrupt contraction and expansion at the upstream and downstream of the lip, respectively. The contraction region is characterized by a laminar flow, which provides the energy and momentum conservation. Whereas in the expansion region, a large value of the Reynolds number implies that the flow comes out from the boundary layer and makes a jet. Therefore, the kinetic energy of the flow dissipates to heat and only momentum is conserved. The combination of the two equations characterizing these states, which share the same mass conservation equation, gives a nonlinear dependence among the three aforementioned variables.

### 3.2 Lip motion equation

The two considered lips vibration models are shown in Figure 7. In both models, each lip is assumed to be a harmonic oscillator with specific values for mass, stiffness, and quality factor. In the transverse model, lip motion is restricted to only the direction perpendicular to airflow and the lip orifice is assumed to have a rectangular shape. The equation governing this model is based on the Bernoulli effect. Whereas in the outward striking model, also called the swinging-door model, the lips execute a swinging motion in the mouthpiece cup.

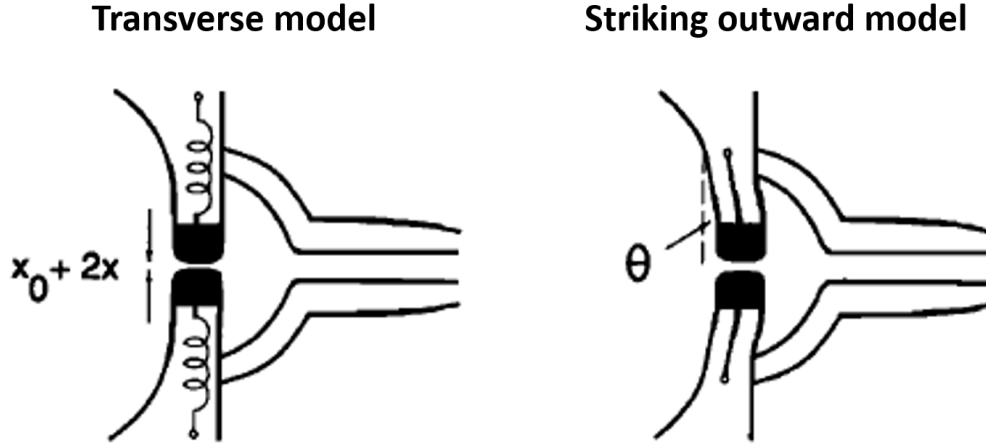


Figure 7: Transverse (on the left) and swinging-door (on the right) lip vibration models

### 3.3 Instrument response equation

As described in Chapter 2, the acoustic properties of the air column are characterized by the input impedance  $Z_{in}(f)$ , which is defined as the ratio of mouthpiece pressure to volume velocity and it is a function of the frequency. This quantity is compared to the characteristic wave impedance  $Z_c$  of an infinite cylindrical tube having the same area at the mouthpiece entry way. This text by Adachi and Sato uses a mathematical model proposed by Schumacher [8] to calculate the acoustic response of the air column, through the use of a reflection function, which is defined by the inverse Fourier transformation of the ratio:

$$\hat{r}(f) = \frac{Z_{in}(f) - Z_c}{Z_{in}(f) + Z_c} \quad (3)$$

Physically, it represents the pressure waveform reflected back to the mouthpiece after the incidence of a pressure impulse to the instrument at the initial time.

The input impedance can be calculated either experimentally or through acoustic relations considering visco-thermal losses. Figure 8 shows the empirically measured input impedance of the paper, similarly to the one found by Benade illustrated in Figure 4. One can observe that the phase of the input impedance is shifted toward negative values at the higher side of the mouthpiece cup's resonance frequency.

### 3.4 Simulation results

Based on the observation by Martin [5], the following assumptions are considered in the model:

- first order approximation of lip vibration model
- linear restoring force, as described by the Hooke's law on the spring
- same vibration amplitude of higher and lower lips
- sinusoidal displacement of the lip orifice
- negligible lip closing time compared to the swing period
- amplitude of the vibration decreases as the frequency increases.



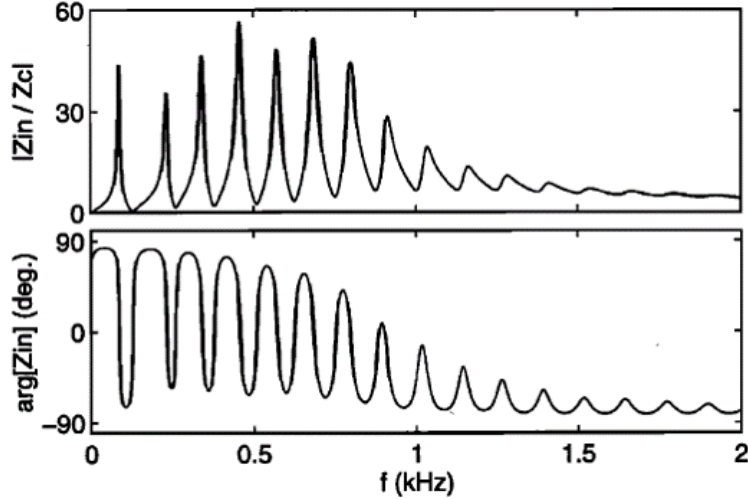


Figure 8: Magnitude and phase angle of input impedance  $Z_{in}$  scaled by the characteristic wave impedance  $Z_c$ , calculated from the shape of a trumpet

Moreover, conditions under which self-oscillation is maintained within a linear theory are considered, which imply a small amplitude of oscillation. With these assumptions, a condition is provided indicating that the oscillation most likely to be generated has a frequency that is near one of the air column resonance frequencies as well as near the lip resonance frequency.

Figure 9 on the left illustrates the behavior of the sound frequency with respect to the lip resonance frequency. With the  $+$  marker the mode frequencies of the input impedance peaks are indicated, while with the  $O$  marker there are the sound production conditions obtained by the simulations for the two models. It can be seen that in the transverse model oscillation is realized on the lower frequency side of the input impedance peaks, while in the swinging-door model oscillation is on the higher frequency side.

On the right of Figure 9, the results of the second resonance mode obtained for the two models are shown. In both lip vibration models, the waveform of the opening of the lips is almost sinusoidal, whereas those of  $p$  and  $U$  contain rich higher harmonics. This is analogous to the oscillation behavior observed in the sound production in the actual brass instruments for loudness levels higher than pianissimo, as explained in Chapter 2.2. The phase relationships among the variables  $p$ ,  $U$ , and  $S_{lip}$  provide the most significant difference between the lip vibration models. The phase of  $p$  is advanced to that of  $U$  for the transverse model, whereas it is retarded for the swinging-door model. So, comparing these results to the curve of the phase of the input impedance illustrated in Figure 8, the swinging door model results to be more suited to simulate the behavior of the brass instrument at lower modes, while the transverse model is more suited for higher modes.

#### 4 *Trumpet sound simulation using a two-dimensional lip vibration model by Seiji Adachi and Masa-Aki Sato*

The previously analyzed article [1] shows that it is impossible to explain in a one-dimensional way the transition from positive phase difference between lip vibration and mouthpiece pressure for lower resonance modes - described by the outward striking model - to negative phase differences for higher modes - described by the transverse model. This paper presents a two-dimensional lip vibration model that can replicate the phase shift relationship by combining the two one-dimensional models. Such a two-dimensional model has

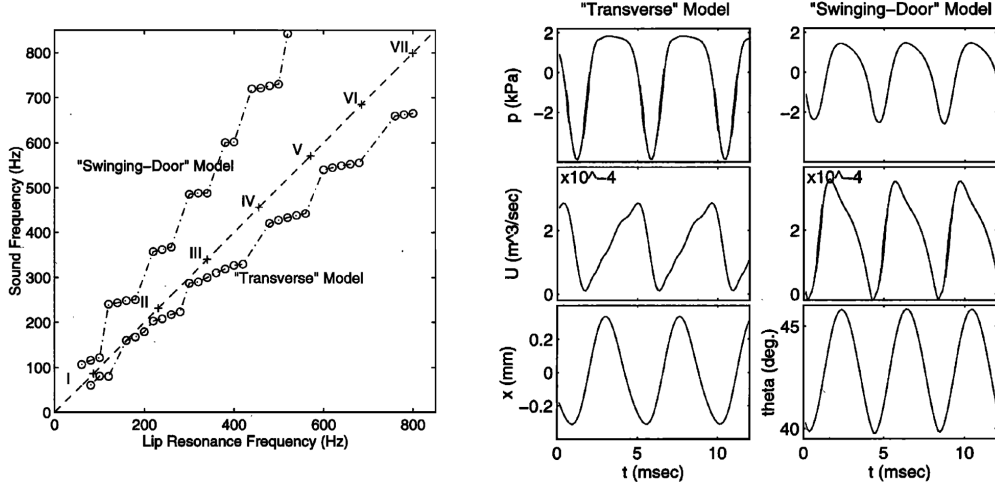


Figure 9: On the left: behavior of the sound frequency with respect to the lip resonance frequency. On the right: waveforms of mouthpiece pressure  $p$ , volume flow rate  $U$ , and lip displacement  $x$  or lip angle  $\theta$  for each lip vibration model

the capability to operate on either frequency side of the input impedance peaks, depending on which of the swinging and stretching motions is dominant.

Figure 10 illustrates the schematic diagram of the two-dimensional lip model. The lip is approximated as a simple mechanical oscillator composed of one mass, stiffness, and damping. It is represented by the parallelogram  $ABCD$  which simultaneously executes both swinging motion with the free joint  $AB$  and stretching motion along the sides  $BC$  and  $AD$ . The two springs supply restoring force for swinging and stretching displacements. The swinging motion is mainly driven by the pressure difference between the player's mouth and the mouthpiece  $p_0 - p$ , whereas the stretching motion is driven by the Bernoulli pressure  $p_{lip}$ .

At a global description level, the model maintains the same system of equations and variables described in Chapter 3, but combining the two one-dimensional models together. In fact, the position of point  $C$  is described by a two-dimensional vector  $\vec{\xi}$  that takes into account both the swinging and the stretching motion, which are balanced by the corresponding restorative forces of the two springs.

In Figure 11, the frequencies of self-excited sound are plotted with  $O$  markers against the lip eigenfrequency. The horizontal dash-dot lines represent the first through sixth resonance frequencies of the instrument. Compared to the results presented in Figure 9, it can be seen that the sounding frequency is not far from the lip eigenfrequency. Moreover, a transition in lip vibration states is observed. The swinging motion dominant oscillation, typical in the lower resonance modes, gives way to the stretching motion dominant oscillation in the higher modes. Frequency gaps between adjacent resonance modes represent the mode transition. In each resonance mode, the sounding frequency does not assume a constant value. Instead, it spans a frequency range, where self-excitation is possible and where the sounding frequency gradually ascends with increases in the lip frequency. In the first, second and third modes, the possible ranges of the sound frequency span both the higher and lower sides of the resonance frequencies, whereas in the fourth, fifth, and sixth modes, they only cover the lower sides.

This theoretically explains why it is much easier to bend the pitch of the sound towards lower frequencies than towards higher frequencies with a brass instrument [6]. This is especially the case for the higher modes than for the lower ones, as can be seen from the Figure 11, and can be easily tested experimentally. Bending is a musical effect sometimes used by brass musicians, in which the player deflects the instrument sound frequency only by varying the lips frequency through the embouchure without changing the length of tubing

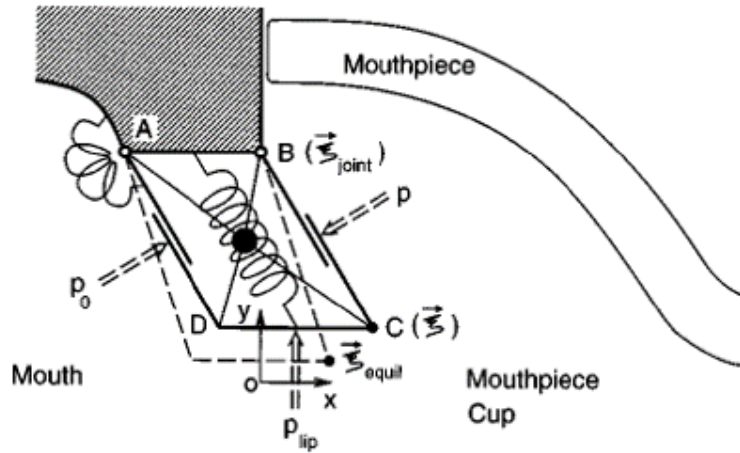


Figure 10: Two-dimensional lip vibration model

(i.e. not changing fingering if playing trumpet or lengthening the slide on a trombone). In fact, it can be easily demonstrated that the range of frequencies accessible with bending towards lower frequencies is much greater than that reachable towards higher frequencies, and that beyond the fourth harmonic it becomes practically impossible to obtain a bending of the sound towards higher frequencies. This is clearly reflected in Figure 11, providing further proof of the model's adequacy to represent the physical system.

## 5 *Nonlinear Dynamics in Physical Models: From Basic Models to True Musical-Instrument Models* by Xavier Rodet and Christophe Vergez

This article by Rodet and Vergez studies the dynamic non-linearity of physical models and proposes an experimentally-tuned basic model of trumpet-like instruments that can reproduce many sound characteristics of the trumpet. It defines a basic scheme of the trumpet model, represented in Figure 12, composed by a loop given by the instrument, characterized by the impulse response of the bore and its corresponding delay, and by another loop given by the interaction between the lips and airflow. It represents a simple system structure which is able to simulate some important characteristics of the timbre of brass instruments, especially in the transients.

The set of variables, equations and assumptions is similar to that of the transverse model of the article by Adachi and Sato discussed in Chapter 3, but in this paper, the Hopf theorem is considered to model the nonlinear coupling of the instrument loop and the lips of the performer. Such theorem allows to prove the existence, uniqueness, and stability of an oscillation around the equilibrium point under study when this equilibrium point becomes unstable. Thus, the frequency and amplitude of the oscillation can be forecasted as a function of a specified bifurcation parameter value, which in this case is represented by the mouth steady pressure. The Hopf theorem provides the circumstances under which the loss of stability of an equilibrium point results in oscillations around this equilibrium point and analyzes such oscillations when a parameter is modified. When the bifurcation parameter becomes greater than a critical value, the system passes from a stable equilibrium point to a locally unique periodic orbit. Such an orbit can be seen as the solution of an order-two harmonic balance, leading to an approximate solution in the lip's displacement, the pressure at the lip, and the airflow through the lips. The theoretical model formulated with the implementation of the Hopf theorem is validated through a comparison with experimental data showing minimal variations in the results.

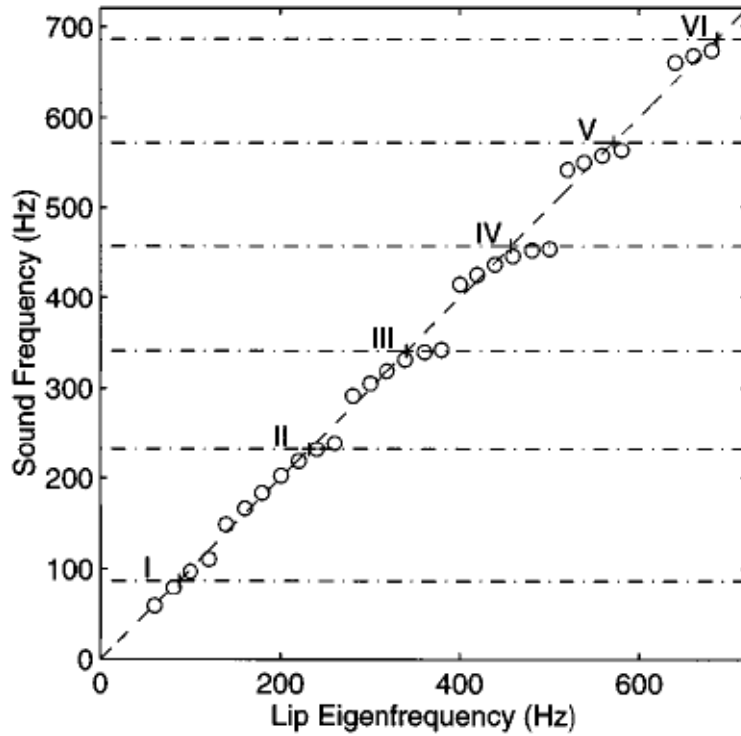


Figure 11: Behavior of the sound frequency with respect to the lip resonance frequency for the two-dimensional model

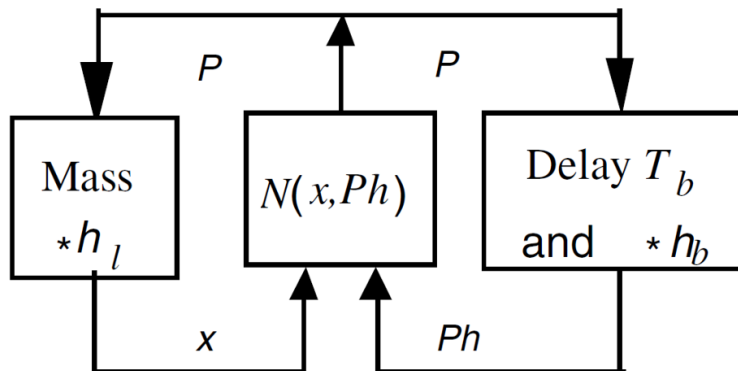


Figure 12: Scheme model of trumpet-like instruments. It is represented by a feedback loop of order two. One loop indicates the feedback of the instrument, characterized by the impulse response  $h_b$  and the time delay of the bore  $T_b$ . Whereas the other loop represents the interaction between the mouthpiece cup and the lips of the musician, that have a non negligible mass and are characterized by the impulse response  $h_l$  and their displacement  $x$ . Both loops affect the pressure level at the lip  $P$

Finally, the article deals with the presence of chaotic signals produced by the instrument and their musical application. The spectrum of most acoustic instruments contains a sinusoidal component and a noise component. The latter is relatively difficult to model in a musically interesting way. If one separately adds noise to a harmonic sound, usually the two signals do not fuse together and the listener perceives them as two separate audio sources. The interest lies in being able to produce a mixed signal, with the sinusoidal and noise components coming from the same process, so that they are perceived as a single sound.

One way to achieve this, based on the observation of the spectrum, is to attribute a harmonic structure to the noise that is dependent on the fundamental frequency of the sound. In this way, the noise component also takes on its own pitch. This can be achieved with the time delayed version of the Chua's circuit, which also allows one to control the proportion of noise in the signal. The paper describes a similar implementation of this method on trumpet's scheme of Figure 12 which proves to be musically promising.

## 6 Conclusions

The aim of this work is to understand the physics behind the production and sound control of brass musical instruments and to study their modeling presented in literature for musical applications. Benade's article analyzes the mechanisms of production of standing waves inside the tube, introduces the definition of wave impedance and anticipates the concept of reflection function. The first described article by Adachi and Sato [1] focuses on describing models that simulate the behavior of the musician's buzzing lips. It analyzes the system by identifying the set of variables and equations involved under specific assumptions. Furthermore, it studies the effects these models generate on the output sound. The second described paper by Adachi and Sato [2] overcomes the limitations of the previous article by describing a system that groups the models described therein. It further highlights the non-linear behavior of the interaction between labial motion and airflow.

Finally, the article by Rodet and Vergez proposes the implementation of the Hopf bifurcation theorem to describe such nonlinearity. Such a mathematical method is applied on a simplified model that simulates the trumpet-like instruments behavior to prove that the system possesses a unique stable periodic orbit when the equilibrium point becomes unstable, and that the characteristics of the oscillating solution are predictable.

# Bibliography

- [1] S. Adachi and M. Sato. Time-domain simulation of sound production in the brass instrument. *Journal of the Acoustical Society of America*, 97:3850–3861, 1995.
- [2] S. Adachi and M. Sato. Trumpet sound simulation using a two-dimensional lip vibration model. *Journal of the Acoustical Society of America*, 99:1200–1209, 1996.
- [3] A. H. Benade. The physics of brasses. *Scientific American*, pages 24–35, July 1973.
- [4] N. H. Fletcher. Autonomous vibration of simple pressure-controlled valves in gas flows. *Journal of the Acoustical Society of America*, 93:2172–2180, 1993.
- [5] D. W. Martin. Lip vibrations in a cornet mouthpiece. *Journal of the Acoustical Society of America*, 13:305–308, 1942.
- [6] M. J. Newton, M. Campbell, J. Chick, and J. A. Kemp. [1] m. j. newton, m. campbell, j. chick, and j. a. kemp, “predicting the playing frequencies of brass instruments. *Proceedings of Forum Acusticum*, pages 1–7, September 2014.
- [7] X. Rodet and C. Vergez. Nonlinear dynamics in physical models: From basic models to true musical-instrument models. *Computer Music Journal*, 23(3):35–49, 1999.
- [8] R. T. Schumacher. Ab initio calculations of the oscillations of a clarinet. *Acoustica*, 48:71–85, 1981.